Design of effectively single-mode air-core photonic bandgap fiber with improved transmission characteristics for the realization of ultimate low loss waveguide

Tadashi Murao, Kunimasa Saitoh, Nikolaos J. Florous, and Masanori Koshiba

Division of Media and Network Technologies, Hokkaido University, Sapporo 060-0814, Japan
murao@icp.ist.hokudai.ac.jp

Abstract: In this paper, we study the novel propagation properties of an improved triangular-type air-core photonic bandgap fiber (PBGF) structured with an anti-resonant silica core surround, through a full-vector modal solver based on the finite-element method (FEM). At first, to realize a single-mode operation over a wide wavelength range, the fiber whose core is constructed by removing 1 air-hole and expanded is proposed and structurally-optimized. In particular, the structural parameters for the fiber that prevent the narrow-band transmission due to the existence of the surface modes and enhance the confinement of the power in the air-core are presented. For the realization of an ultimate low loss transmission, a 7-unit-cell PBGF is analyzed and we show that the 7-unit-cell PBGF can achieve not only lower confinement loss than that of regular-type 7-unit-cell PBGF, but also lower power fraction in the silica-ring when compared with the regular 19-unit-cell PBGF with an anti-resonant core surround, exhibiting an effectively single-mode operation.

OCIS codes: (060.2280) Fiber design and fabrication; (060.2400) Fiber properties; (999.9999) Photonic crystal fiber

References and links

1. P. J. Roberts, T. A. Birks, P. St. J. Russell, T. J. Shepherd, and D. M. Atkin, "Two-dimensional photonic band-gap structures as quasi-metals," Opt. Lett. **21**, 507-509 (1996).
2. R. F. Cregan, B. J. Mangan, J. C. Knight, T. A. Birks, P. S. J. Russell, P. J. Roberts, and D. C. Allan, "Single-mode photonic band gap guidance of light in air," Science **285**, 1537-1539 (1999).
3. J. Broeng, S. E. Barkou, T. Sφndergaard, and A. Bjarklev, "Analysis of air-guiding photonic bandgap fibers," Opt. Lett. **25**, 96-98 (2000).
4. K. Saitoh and M. Koshiba, "Leakage loss and group velocity dispersion in air-core photonic bandgap fibers," Opt. Express **11**, 3100-3109 (2003).
5. C. M. Smith, N. Venkataraman, M. T. Gallagher, D. Müller, J. A. West, N. F. Borrelli, D. C. Allan, and K. W. Koch, "Low-loss hollow-core silica/air photonic bandgap fibre," Nature **424**, 657-659 (2003).
6. K. Saitoh, N. A. Mortensen, and M. Koshiba, "Air-core photonic band-gap fibers: the impact of surface modes," Opt. Express **12**, 394-400 (2004).
7. J. A. West, C. M. Smith, N. F. Borrelli, D. C. Allan, and K. W. Koch, "Surface modes in air-core photonic band-gap fibers," Opt. Express **12**, 1485-1496 (2004).
8. H. K. Kim, J. Shin, S. Fan, M. J. F. Digonnet, and G. S. Kino, "Designing air-core photonic bandgap fibers free of surface modes," IEEE J. Quantum Electron. **40**, 551-556 (2004).
9. H. K. Kim, M. J. F. Digonnet, G. S. Kino, J. Shin, and S. Fan, "Simulations of the effect of the core ring on surface and air-core modes in photonic bandgap fibers," Opt. Express **12**, 3436-3442 (2004).
10. M. Yan and P. Shum, "Air guiding with honeycomb photonic bandgap fiber," IEEE Photon. Technol. Lett. **17**, 64-66 (2005).
11. M. Yan, P. Shum, and J. Hu, "Design of air-guiding honeycomb photonic bandgap fiber," Opt. Lett. **30**, 465-467 (2005).

12. T. Haas, S. Belau, and T. Doll, "Realistic monomode air-core honeycomb photonic bandgap fiber with pockets," J. Lightwave Technol. **23**, 2702-2706 (2005).
13. P. J. Roberts, F. Couny, H. Sabert, B. J. Mangan, D. P. Williams, L. Farr, M. W. Mason, A. Tomlinson, T. A. Birks, J. C. Knight, and P. S. J. Russell, "Ultimate low loss of hollow-core photonic crystal fibres," Opt. Express **13**, 236-244 (2005).
14. P. J. Roberts, D. P. Williams, B. J. Mangan, H. Sabert, F. Couny, W. J. Wadsworth, T. A. Birks, J. C. Knight, and P. St. J. Russell, "Realizing low loss air core photonic crystal fibers by exploiting an antiresonant core surround," Opt. Express **13**, 8277-8285 (2005).
15. N. J. Florous, K. Saitoh, T. Murao, and M. Koshiba, "Non-proximity resonant tunneling in multi-core photonic band gap fibers: An efficient mechanism for engineering highly-selective ultra-narrow band pass splitters," Opt. Express **14**, 4861-4872 (2006).
16. L. Vincetti, F. Poli, and S. Selleri, "Confinement loss and nonlinearity analysis of air-guiding modified honeycomb photonic bandgap fibers," IEEE Photon. Technol. Lett. **18**, 508-510 (2006).
17. T. Murao, K. Saitoh, and M. Koshiba, "Design of air-guiding modified honeycomb photonic band-gap fibers for effectively single-mode operation," Opt. Express **14**, 2404-2412 (2006).
18. P. J. Roberts, D. P. Williams, H. Sabert, B. J. Mangan, D. M. Bird, T. A. Birks, J. C. Knight, and P. St. J. Russell, "Design of low-loss and highly birefringent hollow-core photonic crystal fiber," Opt. Express **14**, 7329-7341 (2006).
19. T. Murao, K. Saitoh, and M. Koshiba, "Realization of single-moded broadband air-guiding photonic bandgap fibers," IEEE Photon. Technol. Lett. **18**, 1666-1668 (2006).
20. R. Amezcua-Correa, N. G. R. Broderick, M. N. Petrovich, F. Poletti, and D. J. Richardson, "Optimizing the usable bandwidth and loss through core design in realistic hollow-core photonic bandgap fibers," Opt. Express **14**, 7974-7985 (2006).
21. K. Saitoh and M. Koshiba, "Full-vectorial imaginary-distance beam propagation method based on a finite element scheme: Application to photonic crystal fibers," IEEE J. Quantum Electron. **38**, 927-933 (2002).
22. K. Saitoh, N. J. Florous, T. Murao, and M. Koshiba, "Design of photonic band gap fibers with suppressed higher-order modes: Towards the development of effectively single mode large hollow-core fiber platforms," Opt. Express **14**, 7342-7352 (2006).
23. M. Yan and P. Shum, "Improved air-silica photonic crystal with a triangular airhole arrangement for hollow-core photonic bandgap fiber design," Opt. Lett. **30**, 1920-1922 (2005).
24. M. J. F. Digonnet, H. K. Kim, G. S. Kino, and S. Fan, "Understanding air-core photonic-bandgap fibers: Analogy to conventional fibers," J. Lightwave Technol. **23**, 4169-4177 (2005).
25. M. A. Duguay, Y. Kokubun, T. L. Koch, and L. Pfeiffer, "Antiresonant reflecting optical waveguides in SiO_2-Si multilayer structures," Appl. Phys. Lett. **49**, 13-15 (1986).
26. N. M. Litchinitser, S. C. Dunn, B. Usner, B. J. Eggleton, T. P. White, R. C. McPhedran, and C. M. de Sterke, "Resonances in microstructured optical waveguides," Opt. Express **11**, 1243-1251 (2003).

1. Introduction

Air-core photonic bandgap fibers (PBGFs), which can be regarded as one of the possible applications for a dielectric quasi-metal structure [1], have gathered much attention in recent years because of their intriguing propagation properties [2-20]. In PBGFs, the incident wave having a longitudinal vector component is reflected when attempting to penetrate into the photonic crystal (PC) cladding. Because the generation of omnidirectional bandgaps is avoided due to the smaller refractive index contrast configuration between glass and air compared with the dielectric quasi-metal case, higher-order modes can be then suppressed effectively. By means of the photonic bandgap (PBG) effect, light can be guided into the air-core with low nonlinearities, and an ultimate low loss property [13, 14], as will be demonstrated also in this study. To realize PBGFs with broadband transmission characteristics and low losses however, the existence of surface modes is the main drawback [5]. When the core and surface modes satisfy the phase matching condition, anti-crossing events occur between these modes [6, 7]. Due to the fact that the scattering loss spectrum of PBGFs exhibits strong peaks, as well as in the case for the confinement loss spectrum at the anti-crossing points between core and surface modes, the attenuation of the guided modes becomes very high over some particular wavelength range near the anti-crossing point, which results in narrow-band transmission in PBGFs. The conditions of the existence of the surface modes are considered as two prominent parts. One is the condition for the PBG cladding [8], where it is necessary to terminate the PC to construct the defected core. When the core radius intersects the corner of the dielectric where the bulk mode has high intensity, the perimeter of the core

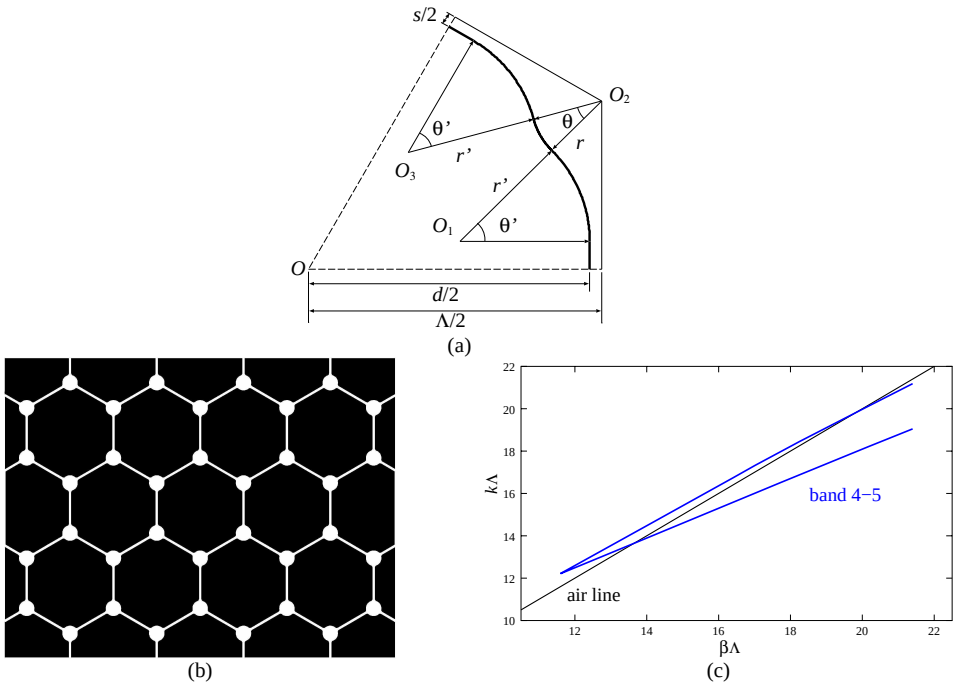

Fig. 1. A portion of the 1/6 region in the unit cell of the improved triangular lattice which consists of air and silica, (b) cladding structure with structural parameters of $d/\Lambda = 0.98$, $r/\Lambda = 0.085$, $\theta = 80.0°$, and (c) PBG diagram for the prescribed structural parameters.

supports surface modes. The second part is associated with the condition for the air-core surround where a silica-ring exists [9] as can be seen in fabricated PBGFs [5]. The width and the radius of the silica-ring are the main factors of dominating the surface modes' condition. If the structural parameters of the silica-ring are appropriately chosen, the modes can be pushed away from the bandgap region and the core mode [20].

When the field intensity at the glass/air interface or light-in-glass power fraction is increased, the scattering losses due to the roughness of the silica-ring surface are enlarged even if the anti-crossing event does not occur. To avoid increasing the overlap integration of the power in the glass, Roberts *et al*. proposed to design the width of the silica-ring around the core to satisfy the first anti-resonant condition at the mid-gap wavelength, in addition to the enlargement of the core radius, by removing 19 air-holes to form the core [14]. Though the loss reduction in the structure has a consequence the reduction of the available operational bandwidth because of the large number of anti-crossing events between core and surface modes, this structure is one of the candidates for the realization of ultimate low loss PBGFs, with the lowest limitation of the loss that has been estimated in Ref. [13]. In the previous reported case however, the optimization of the cladding in terms of reducing the light power fraction in glass was not investigated so far and there is a possibility of reducing the loss further if the other type of cladding is adopted.

In this paper, we adopt the previously-introduced *improved* triangular-type lattice as cladding and we form PBGFs, in which the propagation properties are numerically derived by using a full-vector modal solver based on finite-element method (FEM) [21]. At first, to realize a single-mode operation over a wide wavelength range, the fiber whose core is constructed by removing 1 air-hole and expanded is proposed and structurally-optimized. In particular, the geometrical parameters for the fiber that prevent the narrow-band transmission due to the existence of the surface modes and enhance the confinement of the power into the air-core are presented. As a next step, we study the ultimate low loss properties of a 7-unit-

cell PBGF, and we show that the fiber whose core is realized by removing 7 air-holes can achieve not only lower confinement losses than that of a regular 7-unit-cell PBGF, but also lower power fraction in the silica-ring in comparison with the regular 19-unit-cell PBGF having an anti-resonant core surround, with high power confinement in the air-core when the silica-ring satisfies the first anti-resonant condition at the wavelength in the PBG. Though the higher-order modes exist, because of the large differences of the confinement losses between the fundamental-like mode and the higher-order modes, effectively single-mode operation can be achieved; or in other words, the proposed PBGF can avoid the multi-mode transmission while maintain the low loss level, which is one of the most important issue in air-core PBGFs [22].

2. Modeling of the air-core PBGFs based on the improved triangular lattice

Figure 1(a) shows a portion of the unit cell region in the proposed *"improved"* triangular lattice [23], which consists of air and silica, with d standing for the diameter of the air-holes, Λ is the distance between any of the adjacent air-holes, r is the curvature radius of the orientation of the air-holes, θ is the angle between them, $n_1 = 1.0$ and $n_2 = 1.45$ are the refractive indices of air and silica, respectively. When this set of structural parameters is defined, the cladding structure is well described; in fact, s, θ', r', and x-y coordinates of O_1 shown in Fig. 1(a) can be calculated using the following formulas:

$$s = \Lambda - d \,, \tag{1}$$

$$\theta' = 30^\circ + \frac{\theta}{2}, \tag{2}$$

$$r' = \frac{r\cos\theta' - s/2}{1-\cos\theta'}, \tag{3}$$

$$O_{1x} = \frac{d}{2} - r', \tag{4}$$

$$O_{1y} = \frac{\Lambda}{2\sqrt{3}} - \left(r' + \frac{s}{2}\right)\tan\theta' . \tag{5}$$

Because the optimization of this structure has been performed to some extent in Ref. [23], the following values are chosen as structural parameters: $d/\Lambda = 0.98$, $r/\Lambda = 0.085$, and $\theta = 80.0°$. By employing such parameters, the improvement of the narrow-band transmission caused by the anti-crossing phenomenon between the core and the surface modes, takes place. In Figs. 1(b) and (c), we show the cladding structure and the $\beta\Lambda$-dependence of the bandgap of the light for the out-of-plane propagation for the *improved* triangular lattice with $d/\Lambda = 0.98$, $r/\Lambda = 0.085$, and $\theta = 80.0°$ calculated by using FEM, where β stands for the propagation constant and k for the wavenumber in free space. The relative bandgap size is enhanced by a factor of 1.2 when compared with the regular triangular lattice with $d/\Lambda = 0.98$ (hexagonal air-holes with rounded corners). When large bandgaps are obtained in the cladding, low confinement losses as well as broadband transmission characteristics are expected [10, 11, 16, 17].

3. Single-mode air-core PBGF based on the improved triangular-type cladding

Figures 2(a) and (b) show the cross sections of the two defected core types, which are named 1-unit-cell PBGF and 7-unit-cell PBGF, respectively. In order to realize a single-mode operation over a wide wavelength range, we consider the fiber whose core is constructed by removing 1 air-hole and expanded, as shown in Fig. 2(a). At first, in this section, we show that the reduction of the core-radius in this type of PBGFs with a silica core surround can enhance the confinement in the PBG region, which generally results in multi-mode operation contrary

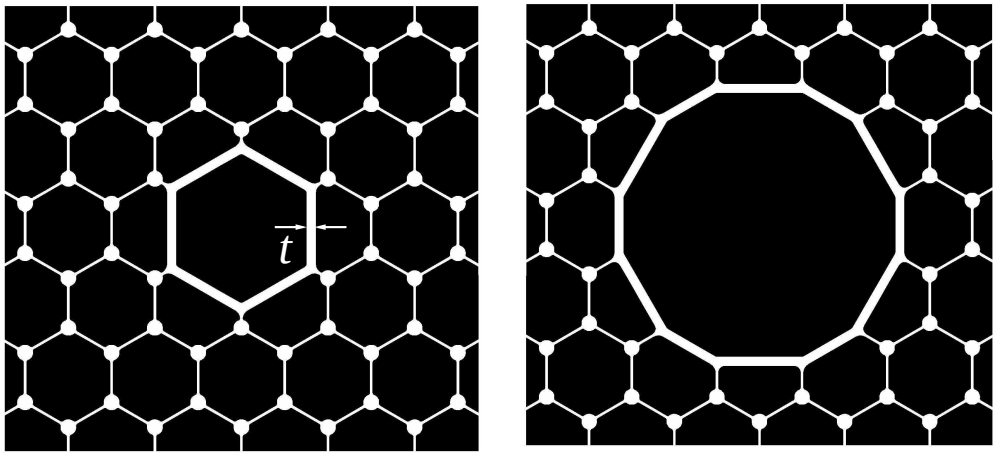

(a) (b)

Fig. 2. Cross sections of the proposed PBGFs whose defected cores are realized (a) by removing 1 air hole and expanded (core radius $R \approx 3.2$ μm), and (b) by removing 7 air-holes ($R \approx 6.4$ μm). In both cases, the structural parameters of the cladding are $d/\Lambda = 0.98$, $r/\Lambda = 0.085$, $\theta = 80.0°$, and $\Lambda = 4.0$ μm.

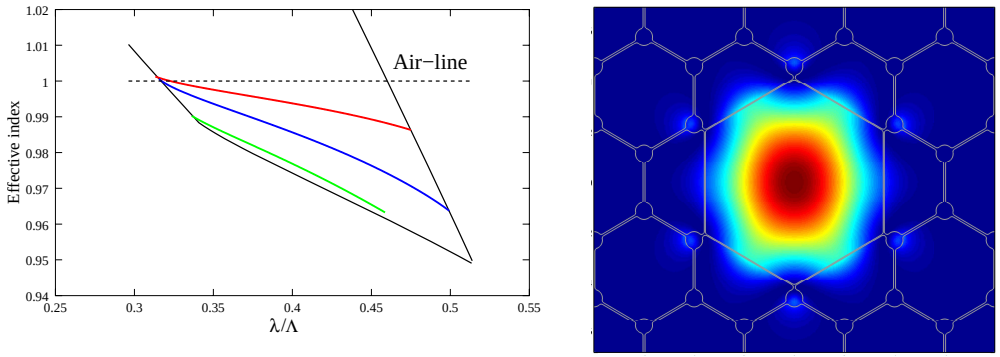

(a) (b)

Fig. 3. (a) Effective refractive indices of the guided modes as a function of normalized wavelength for the fiber whose core is realized by removing 1 air-hole and expanded, with normalized silica-ring thickness $t/\Lambda = 0.01$. The black solid curves represent the PBG boundaries. The fundamental mode is represented by the red curve, the second-order mode by the blue curve, and the third-order mode by the green curve. (b) Surface plots for the *z*-component of the Poynting vector for the fundamental-like mode at normalized wavelength of $\lambda/\Lambda = 0.4$.

to the index-guiding conventional fibers. Then the condition for achieving the desired single-mode operation is investigated in a detailed manner and we numerically show that when the silica-ring is designed to satisfy the first anti-resonant condition, the PBGF with a realistic core can operate in a single-mode fashion over 400 nm wavelength range. At this point we should clarify that although the bandgap properties of the proposed cladding type have been already reported, there is no any attempt so far as to incorporate this type of cladding in order to form a realistic PBGF. From this point of view our investigation may be considered novel and useful to the fiber community.

Figure 3(a) shows the effective refractive indices of the guided modes as a function of the normalized wavelength λ/Λ, for the fiber with a thin silica core surround of normalized thickness $t/\Lambda = 0.01$. The black solid curves represent the PBG boundaries for the *improved* triangular lattice, provided that the number of cladding rings is infinite. Here, only the HE_{21}-

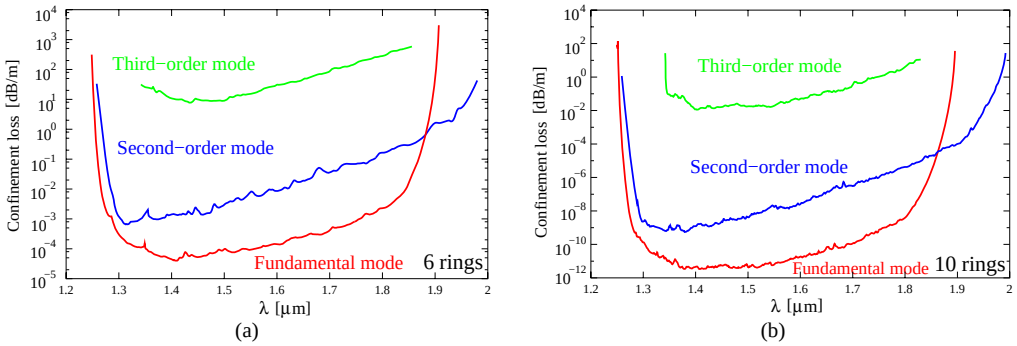

Fig. 4. Confinement losses of the fiber whose core is realized by removing 1 air-hole and expanded for (a) 6 rings (b) 10 rings. In both cases, $t = 0.01\Lambda$ and $\Lambda = 4.0$ μm.

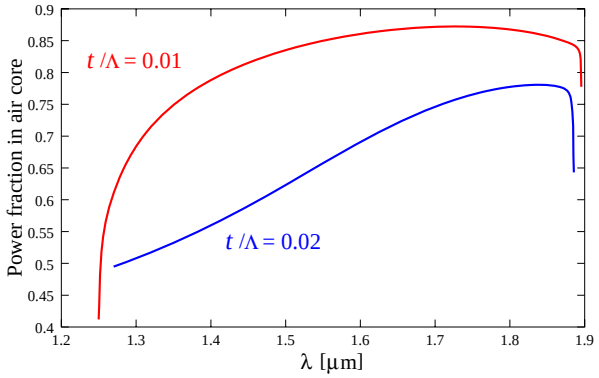

Fig. 5. The wavelength dependence of the power fraction in the air-core of the fundamental-like mode for PBGF with $t = 0.01\Lambda$ (red curve), and $t = 0.02\Lambda$ (blue curve), where $\Lambda = 4.0$ μm.

like mode is shown as the second-order mode, because the effective indices of the TM_{01}-like and TE_{01}-like modes were found to be close between each other while only the EH_{11}-like mode is shown as the third-order mode for the same reason. The fundamental-like mode exists inside the bandgap region, while the lower and higher cutoff wavelengths are $\lambda/\Lambda = 0.313$ and $\lambda/\Lambda = 0.475$, respectively. In Fig. 3(b), we present a surface plot for the *z*-component of the Poynting vector, for the fundamental-like mode at a normalized wavelength of $\lambda/\Lambda = 0.4$. In spite of the sufficient small core-radius that was employed in order to realize the single-mode operation, higher-order modes co-exist inside the bandgap region, though the maximum number of core modes was approximately estimated to be 5.4 (including the degenerated modes), according to the analogous theory of conventional fibers [24]. In Fig. 3(a), the effective index of the fundamental-like mode exceeds the limit of waves that can propagate in free space (the upper air-line is the boundary for air), particularly at shorter wavelength range. Although the fundamental mode is confined in the air-core to some extent in this wavelength range, due to the fact that the mode penetrates the silica-ring, the effective index of the fundamental mode is found to be greater than one. Figures 4(a) and (b) show the wavelength-dependence of the confinement losses for the fiber with six and ten cell-rings. In our calculations, regarding the confinement loss curves presented in this manuscript, a resolution in the wavelength span of about 0.25 nm was used, a value which can be fairly considered low enough. In addition the mesh size used for discretizing the structure in our calculations was very fine (e.g., number of 500,000 unknowns was used for the 10-rings fiber structure case). Even in this case however, the obtained results seem a bit noisy, a fact that shows according to our interpretation that the origin of the noise in the confinement loss curves is not directly

related with the numerical resolution of our calculations. So the origin of the noise may be related with some physical mechanism of small oscillations coming most probable from the silica-ring. Due to the interaction of the light with the silica core surround, the effective indices of the modes and the confinement of the light in the PBG region increase, which lead to multi-mode operation, as well as the lower confinement losses for the modes because the dispersion curves appear to be more centered in the PBG region. In Fig. 5 we compare the wavelength dependence of the power fraction in the air-core of the fundamental-like mode, for the PBGF with $t = 0.01\Lambda$ (red curve) and $t = 0.02\Lambda$ (blue curve), where $\Lambda = 4.0$ μm. The confinement of the power in the air-core in this case is relatively low due to the small size of the core; in addition, the mode is strongly affected by the presence of the silica core surround as can be seen in Figs. 3. In this case, although the confinement losses for the modes are low, in practice, the attenuations are expected to be very high because of the scattering losses due to the roughness between the silica/air surfaces.

The key to reduce the influence of the silica-ring around the core and to further realize a high confinement of the light in the air-core is the employment of a mimic anti-resonant reflective optical waveguide (ARROW) for the silica-ring, proposed recently by Roberts *et al* [14]. Anti-resonant reflection [25] for an operating wavelength-λ reaches the minimum value for the high index inclusion "waveguide" around the air-core which supports new modes, or in other words, satisfies the modal cutoff condition [26]. On the other hand, the reflection for a wavelength-λ reaches the maximum value for the silica-ring that satisfies the following condition:

$$t = \frac{(2N+1)\lambda}{4\sqrt{n_2^2 - 1 + \left(\lambda/4R\right)^2}}, \quad N = 0, 1, 2, ... \tag{6}$$

where t is the width of the silica-ring and R is the core radius of the fiber. In particular for the fundamental mode, the approximation $\left(\lambda/4R\right)^2 << 1$ can be applied in this equation. Although the modal behavior is expected to change, we consider the case for only the first anti-resonant condition, because the width of the silica-ring for higher-order anti-resonant condition is relatively thicker.

Figure 6(a) shows the dispersion curves as a function of the wavelength for the fiber shown in Fig. 2(a), where the thickness of the silica-ring was chosen to be $t/\Lambda = 0.095$ in order to satisfy the first anti-resonant condition at the mid-gap wavelength. The black solid curves represent the PBG boundaries provided that the number of the cladding rings is infinite. Only the fundamental-like mode exists in the bandgap region as the air-core mode, and the lower and higher cutoff wavelengths are $\lambda/\Lambda = 0.351$ and $\lambda/\Lambda = 0.501$, respectively. Because of the reduction of the silica effect on the modes, the dispersion curves of the air-core modes shift down relatively to the position of the air-line, an effect which results in the suppression of the higher-order modes. Although several anti-crossing points exist between core and surface modes, due to the large bandgap in the cladding the narrow-band transmission is prevented. In Fig. 6(b), we show the surface plot for the *z*-component of the Poynting vector, for the fundamental-like mode at a normalized wavelength of $\lambda/\Lambda = 0.4$. The mode is well-confined in the air-core region. Figures 7(a) and (b) show the wavelength-dependence of the confinement losses for the fiber with a total number of six and ten rings, respectively, where the pitch constant was chosen as $\Lambda = 4.0$ μm in order to operate in the telecommunication window (e.g., around 1.55 μm in wavelength). Although the confinement losses are a little bit higher than in the case for $t = 0.01\Lambda$ because of the down-shift of the dispersion curves, the PBGF with an anti-resonant silica-ring exhibits a single-mode operation with low confinement losses over a wide wavelength range. In Fig. 8(a), we show the wavelength-dependence of the power fraction in the air-core for the fundamental-like mode for the PBGF with $t/\Lambda = 0.095$. High confinement of the power in the air-core can be clearly observed. Figure 8(b) shows the

wavelength-dependence of the η-factor [14], where η-factor is defined as the normalized overlap integration of the power in the silica-ring as follows:

$$\eta = \left| \frac{\int_{\text{glass annulus}} dA\, \boldsymbol{E} \times \boldsymbol{H}^* \cdot \boldsymbol{z}}{\int_{\text{cross-section}} dA\, \boldsymbol{E} \times \boldsymbol{H}^* \cdot \boldsymbol{z}} \right|. \tag{7}$$

In spite of its small core radius, a relatively low η-factor was obtained, which lead to the guidance of light with low attenuation. In Figs. 9(a) and (b), we show the power fraction in the air-core and the η-factor as a function of the silica-ring thickness with the first anti-resonant condition over PBG regions, as well as the wavelength. In these figures, the yellow diagonal regions in Fig. 9(a) and watery diagonal regions in Fig. 9(b) correspond to anti-crossings between core and surface modes. By considering the high power confinement in the air-core, the lower η-factor and the wide operational wavelength range, if we design the silica-ring thickness around t/Λ = 0.108 – 0.115, the optimum device performance can be achieved. For example, if t/Λ = 0.108, the η-factor is 0.0076. Surprisingly, in spite of its small core radius, the η-factor was found to be lower than the corresponding regular 7-unit-cell triangular-type PBGF (see Fig. 7(b), with no core ellipses in Ref. [18]). This implies that there is a possibility to further reduce the η-factor in PBGFs by optimizing the cladding structure, in spite from the fact that optimizations have been investigated so far focusing only on the air-core perimeter [14, 18, 20].

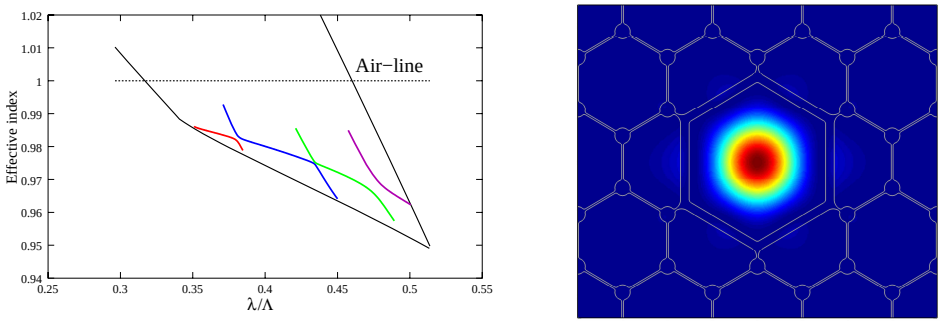

Fig. 6. (a) Effective refractive indices of the guided modes as a function of the normalized wavelength for the fiber whose core is realized by removing 1 air-hole and expanded, where t/Λ = 0.095, satisfying the first anti-resonant condition. (b) Surface plot for the z-component of the Poynting vector for the fundamental-like mode at a normalized wavelength of λ/Λ = 0.4.

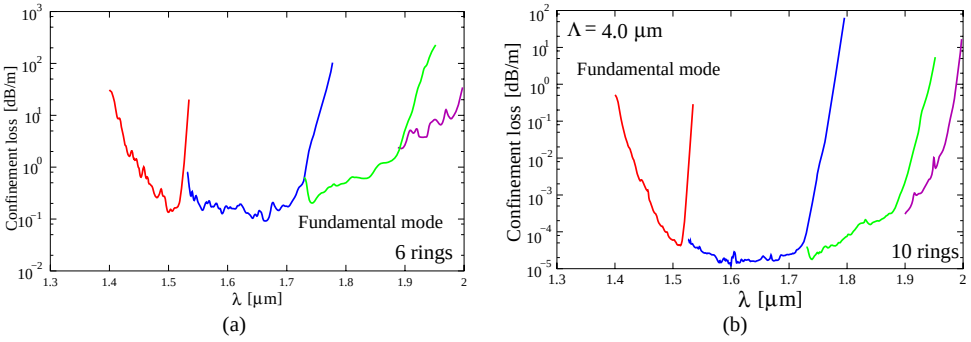

Fig. 7. Confinement losses of the fiber whose core is realized by removing 1 air-hole and expanded for (a) 6 rings (b) 10 rings. In both cases, t = 0.095Λ and Λ = 4.0 μm.

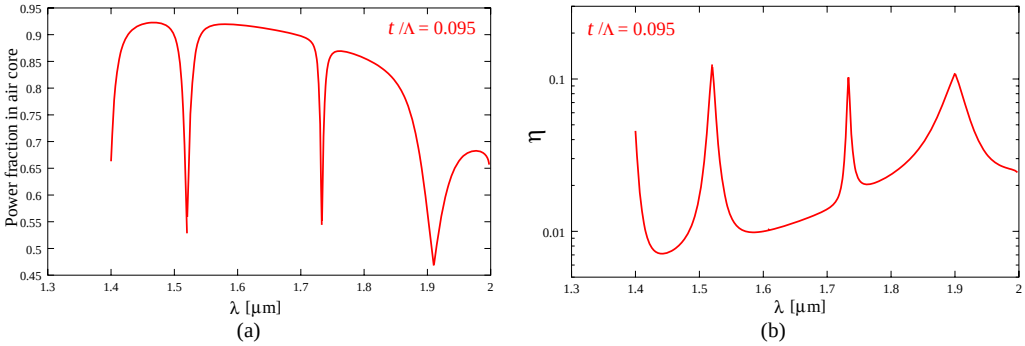

Fig. 8. The wavelength-dependence of the power fraction in (a) the air-core, and (b) the silica-ring for the fundamental-like mode of the proposed PBGF whose core is realized by removing 1 air-hole and expanded, with d/Λ = 0.98, r/Λ = 0.085, θ = 80.0°, t = 0.095Λ, and Λ = 4.0 μm.

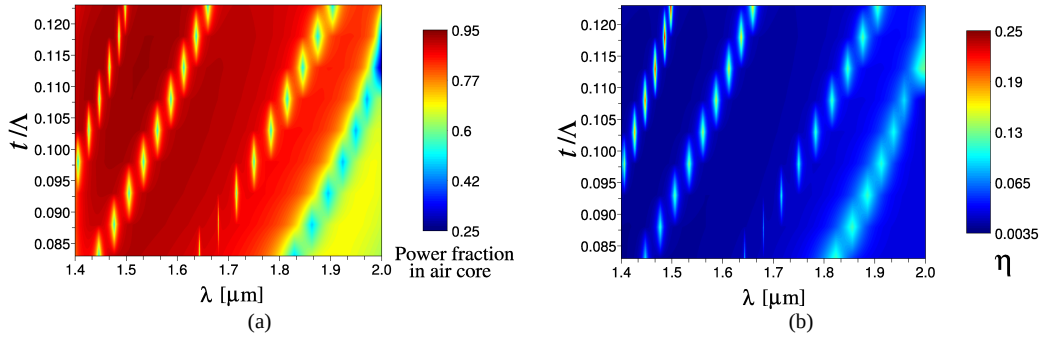

Fig. 9. Variation color-map of the power fraction in (a) the air-core, and (b) the silica-ring for the fundamental-like mode of the PBGF, with d/Λ = 0.98, r/Λ = 0.085, θ = 80.0°, and Λ = 4.0 μm.

4. PBGFs with ultimate low loss transmission characteristics

In order to realize an ultimate low-loss transmission, we consider the 7-unit-cell PBGF with the improved triangular-type cladding as shown in Fig. 2(b), where the thickness of the silica-ring is chosen as t/Λ = 0.095 in order to satisfy the first anti-resonant condition at the mid-gap wavelength. Figure 10(a) shows the dispersion curves as a function of the wavelength for the fiber shown in Fig. 2(b). Here, only the HE_{21}-like and TE_{01}-like modes are shown as second-order modes, because the effective index of the TM_{01}-like mode was found to be close to the HE_{21}-like and TE_{01}-like modes, while only the HE_{31}-like and EH_{11}-like modes are shown as the third-order modes for the same reason. The black solid curves represent the PBG boundaries. The fundamental-like mode exists inside the bandgap region while the lower and higher cutoff wavelengths were found to be λ/Λ = 0.322 and λ/Λ = 0.469, respectively. Due to the large core radius, higher-order modes (dilute red curves) co-exist in the PBG region, as can also be seen in regular triangular-type PBGFs [6]. In Fig. 10(b), we show the surface plots for the z-component of the Poynting vector, for the fundamental-like mode at a normalized operational wavelength of λ/Λ=0.4. The mode is well-confined in the air-core region. Figures 11(a) and (b) show the wavelength dependence of the confinement losses of the HE_{11}-like, HE_{21}-like, TE_{01}-like, HE_{31}-like, and EH_{11}-like modes for the fiber with a total number of six rings, where Λ = 4.0 μm. The confinement loss for the fundamental-like mode is very low and we note that this value is about 1-order of magnitude smaller than that observed in regular triangular-type PBGFs with d/Λ = 0.98 with the same number of cladding rings [6]. Although the confinement losses for the higher-order modes as well as that of the fundamental-like

mode are relatively low, we can find some differences in the characteristics of the confinement losses between fundamental and higher-order modes. In particular, for this type of fiber, the confinement loss of the fundamental-like mode performs like a "well" as a function of wavelength; that is, it does not increase rapidly even if the wavelength lies near the bandgap edges in contrast to higher-order modes, and cannot be seen in the other type of air-core PBGFs. Because of this unusual characteristic, only the fundamental-like mode is guided in the core without surface modes around 1.32 μm – 1.46 μm, suppressing the higher-order mode, which can potentially lead to effectively single-mode operation (actually it can be achieved by reducing the number of cladding rings from 6 to 5, as it will be shown later). The confinement losses of the second-order mode are actually about 2-orders of magnitude larger than that of the fundamental-like mode at shorter wavelengths. This result is comparable to what can be achieved in Ref. [22]. As a consequence, this novel type of PBGF can avoid the multi-mode transmission while being consistent with the requirement for the ultimate low-loss transmission, which is one of the main drawbacks in air-core PBGFs. In addition, this short wavelength operation, is better in terms of enhancing the power fraction into the air-core and further reducing the η-factor for this type of PBGF as will be described later. In Fig. 12(a), we show the wavelength dependence of the power fraction in the air-core of the fundamental-like mode for the *improved* triangular-type 7-unit-cell PBGF with $t/\Lambda = 0.095$. High confinement of the power in the air-core can be achieved and the highest value attained for this fiber is 99.43% at a wavelength of 1.39 μm. This is noticeable because what can be attained in regular triangular-type 7-unit-cell air-core PBGFs is not more than 98%, even for the structural parameter $d/\Lambda = 0.98$ with realistic claddings (hexagonal air-holes with rounded corners). The value which can be achieved in the proposed fiber is in fact closer to that of regular triangular-type 19-unit-cell air-core PBGFs with the structural parameter of $d/\Lambda = 0.98$ (hexagonal air-holes with rounded corners), while the core radius of the proposed fiber is almost the same as that in the regular triangular-type 7-unit-cell PBGFs. Figure 12(b) shows the wavelength-dependence of the η-factor for the improved triangular-type 7-unit-cell PBGF with $t/\Lambda = 0.095$. We note that the value obtained can be considered very low and the lowest value attained for this fiber is 0.0011 at a wavelength of 1.38 μm, which is comparable to what can be achieved in triangular-type 19-unit-cell air-core PBGFs with anti-resonant core surround in Ref. [14]. This wavelength corresponds to the suppressed higher-order mode range, therefore, ultra-low loss transmission with effectively single-mode operation can be observed.

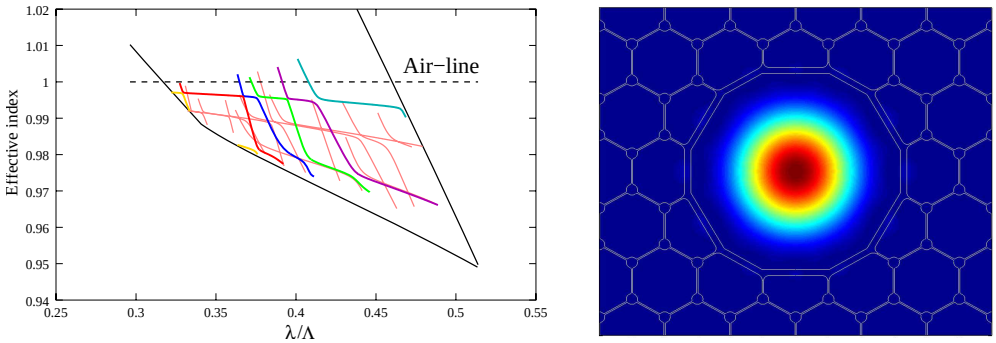

(a) (b)

Fig. 10. (a) Effective refractive indices of the guided modes as a function of normalized wavelength for the fiber whose core is realized by removing 7 air-holes, where $t/\Lambda = 0.095$ to satisfy the anti-resonant condition. (b) Surface plots for the *z*-component of the Poynting vector for the fundamental-like mode at normalized wavelength of $\lambda/\Lambda = 0.4$.

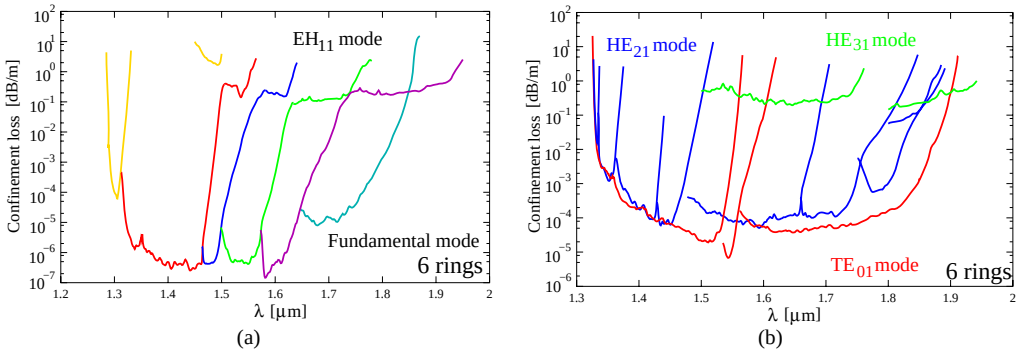

Fig. 11. Confinement losses of the fiber whose core is realized by removing 7 air-holes for 6 rings for (a) the fundamental-like and EH_{11}-like modes, and (b) for the HE_{21}-like, TE_{01}-like, and HE_{31}-like modes, where Λ = 4.0 μm and t/Λ = 0.095 to satisfy the anti-resonant condition.

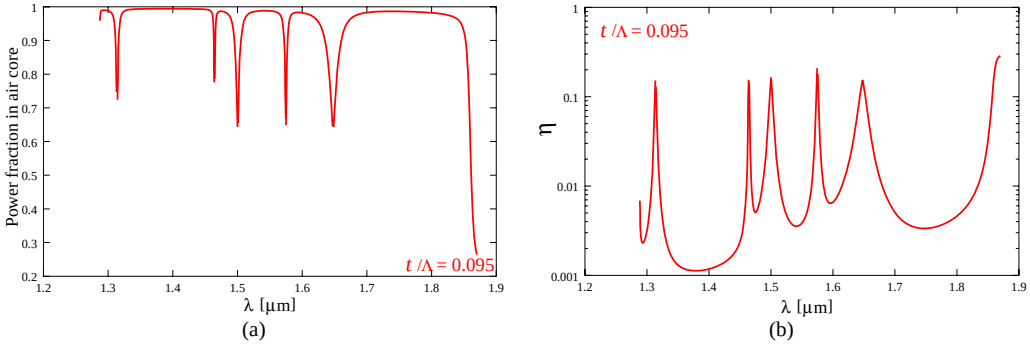

Fig. 12. The wavelength dependence of the power fraction (a) in the air-core, and (b) in the silica-ring for the fundamental-like mode of the proposed PBGF whose core is realized by removing 7 air-holes with d/Λ = 0.98, r/Λ = 0.085, θ = 80.0°, t = 0.095Λ, and Λ = 4.0 μm.

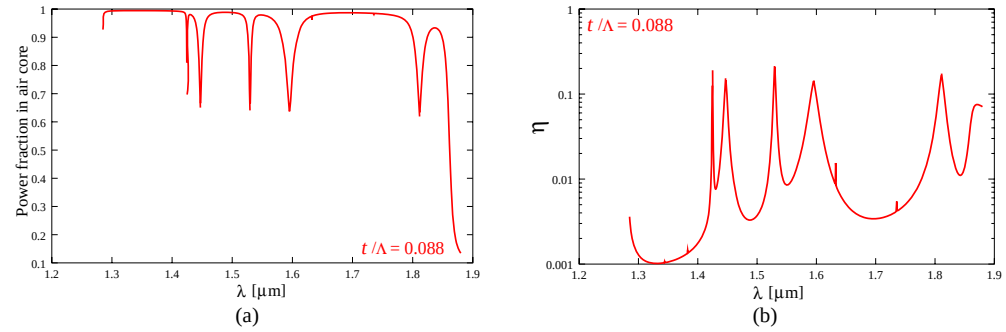

Fig. 13. The wavelength dependence of the power fraction (a) in the air-core, and (b) in the silica-ring for the fundamental-like mode of the proposed PBGF whose core is realized by removing 7 air-holes with d/Λ = 0.98, r/Λ = 0.085, θ = 80.0°, t = 0.088Λ, and Λ = 4.0 μm.

In order to realize further "ultimate low loss" fiber, we consider an optimized structure that realizes the higher power confinement in the air-core, the lower η-factor, while at the same time is keeping the effectively single-mode operation. We note that the wavelength of the anti-crossing points between core and surface modes shifts toward shorter wavelengths by decreasing the width of silica-ring, as seen above and also confirmed in Ref. [20]. In addition the reduction of the width of the silica-ring leads to the enhancement of the power

confinement in the air-core and further reduces the η-factor in this type of PBGF as can be seen in Figs. 9. By considering the previous two reasons, we conclude that we have to design the silica-ring to satisfy the first anti-resonant condition, not in mid-gap wavelength but in a relatively shorter wavelength 1.48 μm (in this case, keeping the rest of the geometrical parameters as constants). Figure 13(a) shows the wavelength-dependence of the power fraction in the air-core of the fundamental-like mode for the *improved* triangular-type 7-unit-cell PBGF with $t/\Lambda = 0.088$. Higher confinement of the power in the air-core can be achieved and the highest value attained for this fiber is 99.45% at 1.34 μm wavelength. Figure 13(b) shows the wavelength-dependence of the η-factor for the improved triangular-type 7-unit-cell PBGF with $t/\Lambda = 0.088$. We note that the lowest value attained for this fiber is 0.0010 at 1.33 μm wavelength, which is 1.2 times lower than the minimum found in the triangular-type 19-unit-cell air-core PBGFs with an anti-resonant core surround [14]. In Fig. 14, we show the confinement losses as a function of the wavelength for the improved triangular-type 7-unit-cell PBGF with $t/\Lambda = 0.088$ and 5 cladding rings. Here, only the TE_{01}-like mode is shown as the second-order mode. Because of the difference of confinement losses between fundamental and second-order mode as well as the fact that the highest power fraction into the air-core and lowest η-factor are attainable in the shorter wavelength range for the fundamental-like mode, this novel type of PBGF operates as an effectively single-moded while at the same time is consistent with the ultimate low-loss transmission in the grey strip region.

Although in this study we have considered only the 7-unit-cell PBGFs, if we consider a PBGF whose core is realized by 19 air-holes, further loss reduction, higher power confinement in the air-core, and the lower η-factor is expected to be observed. In this case, however, the fiber may suffer from multi-mode operation. The objective of this paper was to realize an ultimate low loss fiber without increasing the core size in order to suppress the higher-order modes and also to realize a robust platform to possible bending operation of the fiber. Recently, a PBGF whose silica-ring is constructed by arrangements of cylinders evenly distributed around a circle was proposed [18]. If the proposed structure is incorporated into our PBGF, much lower attenuation as well as higher confinement of the power in the air-core and broadband transmission due to the existence of fewer surface modes is expected. Although the purpose of this paper was the theoretical investigation of the propagation properties of air-guiding PBGFs, at this point we would like to comment on the feasibility of our proposed PBGF. Perhaps at this stage the fabrication technologies may not be appropriate for constructing improved triangular PC lattices. In particular, there exists an issue concerning the microstructural control for the θ-parameter. According to Fig. 4 and Fig. 6 of Ref. [23], however, the PBGF performance does not change so drastically for a small variation of the θ-parameter. Though the performance changes for a small variation of the solid silica rod diameter-*r*, which would be inserted at the confluence between three silica tubes, it is more crucial that this parameter is considered to be easily controlled. By considering the previous two reasons, it can be estimated that the performances change of the actual fabricated fiber will be relatively small. We strongly believe that in the near future with more advanced fabrication techniques the construction of this PBGF will become possible [23].

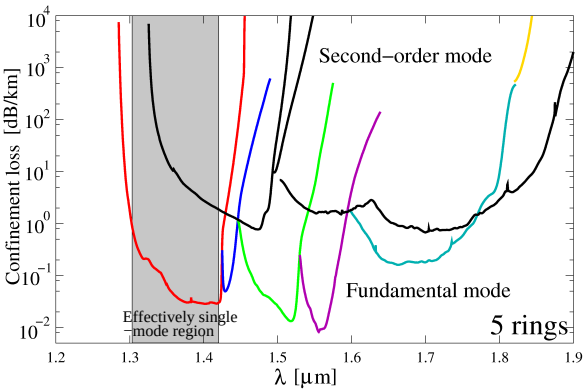

Fig. 14. Confinement losses of the fiber whose core is realized by removing 7 air-holes, and having 5 air-hole rings for the fundamental-like (red, blue, green, purple, cyan, and yellow curves) and second-order modes (black curves), where Λ = 4.0 μm and t/Λ = 0.088 to satisfy the anti-resonant condition at the wavelength of 1.48 μm.

5. Conclusions

To conclude our work, at first, we have proposed and optimized an effectively single-mode air-core PBGF based on an *improved* triangular-type cladding, whose core is realized by removing 1 air-hole and expanded, in terms of power fraction in the air-core and in the silica-ring. In particular, the structural parameters for the fiber that prevent narrow-band transmission due to the existence of the surface modes and further enhance the confinement of the power in air-core have been presented. The realization of an ultimate low loss transmission, in 7-unit-cell PBGF has also been presented by incorporating the prescribed *improved* triangular lattice cladding. The fiber whose core is realized by removing 7 air-holes can achieve not only the lowest confinement loss when compared to that of the regular triangular-type 7-unit-cell PBGF (hexagonal air-holes), but also lower power fraction in the silica-ring than even in the regular triangular-type 19-unit-cell PBGF (hexagonal air-holes) having an anti-resonant core surround, with simultaneous improvement in the high power confinement in the air-core, when the silica-ring satisfies the first anti-resonant condition at a wavelength in the PBG. Though the higher-order modes exist, because of the large differences of the confinement losses between the fundamental-like mode and higher-order modes, effectively single-mode operation can be achieved, a result which was found to be consistent with the requirement for ultimate low loss transmission, which is one of the most challenging technical issues in air-core PBGFs.